Cement and Concrete Research 40 (2010) 778–786

Contents lists available at ScienceDirect

Cement and Concrete Research

journal homepage: http://ees.elsevier.com/CEMCON/default.asp

Re-use of drinking water treatment plant (DWTP) sludge: Characterization and technological behaviour of cement mortars with atomized sludge additions

N. Husillos Rodríguez [a,*], S. Martínez Ramírez [a], M.T. Blanco Varela [a], M. Guillem [b], J. Puig [b], E. Larrotcha [c], J. Flores [c]

[a] Instituto de Ciencias de la Construcción Eduardo Torroja (CSIC), Serrano Galvache 4, 28033 Madrid, Spain
[b] Cementos Molins S.A., Crta. N-340, 2 al 38, E-08620 Sant Vicenç dels Horts, Barcelona, Spain
[c] Aguas de Barcelona S.A., Avenida Diagonal 211, 08018 Barcelona, Spain

ARTICLE INFO

Article history:
Received 2 June 2009
Accepted 23 November 2009

Keywords:
Waste management (E)
DWTP sludge
Cement (D)
Mortar (E)
Calorimetry (A)

ABSTRACT

This paper aims to characterize spray-dried DWTP sludge and evaluate its possible use as an addition for the cement industry. It describes the physical, chemical and micro-structural characterization of the sludge as well as the effect of its addition to Portland cements on the hydration, water demand, setting and mechanical strength of standardized mortars.

Spray drying DWTP sludge generates a readily handled powdery material whose particle size is similar to those of Portland cement. The atomized sludge contains 12–14% organic matter (mainly fatty acids), while its main mineral constituents are muscovite, quartz, calcite, dolomite and seraphinite (or clinoclor). Its amorphous material content is 35%.

The mortars were made with type CEM I Portland cement mixed with 10 to 30% atomized sludge exhibited lower mechanical strength than the control cement and a decline in slump. Setting was also altered in the blended cements with respect to the control.

1. Introduction

The sludge removed from drinking and waste water treatment plants generates growing amounts of waste, which have to be managed. The total production of sewage sludge for the United States of America (USA) and countries of the European Union (EU) approaches 17 Mt of dry solids per year (7 Mt in USA + 10 Mt in EU) [1].

The sludge management process in place at Aguas de Barcelona's San Joan Despí DWTP comprises the following stages: sludge gathering and storage, pumping to thickening area, thickening, storage of thickened sludge, pumping to dehydration area, dehydration, atomization and final storage [2].

Atomization, which aims to obtain a semi-fine, highly fluid product with residual moisture of under 5%, consists in a rotary co-current system with a maximum evaporation capacity of 3000 kg/h.

The use of the atomization system described allows us: a) the re-use of sludge generated in treatment plants as a prime material in industrial processes; b) The preservation of natural spaces by avoiding the final destination of sludge in landfills, c) the reduction of area devoted to the on site storage of such waste, as well as substantial savings in transport costs.

A considerable portion of the DWTP waste generated in Spain is deposited in dumps. Spray drying this sludge would reduce the volume by 75% and generate a dry, more readily handled product, whose re-use in the cement industry is explored in the present study.

Since the volume of sewage sludge (SS) is much greater than DWTP sludge, more information is available and much more research has been conducted on the former. One way to recycle this waste would be to add the original sludge or the ash from its incineration to cement or concrete.

According to Cyr et al. [3], 22% of the sludge produced in the USA and 15% produced in Europe is incinerated, creating a need to manage the 1.2 Mt of ash (SSA) generated. A number of researchers have studied the pozzolanic capacity of this ash [4–8], the properties of the mortars and concretes made with the cements containing it [9–15] and the heavy metal containment capacity of the cementitious matrices [16–20]. The direct addition of SS to concrete has also been studied and its effect on setting, strength, leaching and so forth has been determined [21–23].

This study aimed to characterize DWTP sludge atomized as described and evaluate its possible use as addition for the cement industry. This study describes the physical, chemical and micro-structural characterization of the sludge and the effect exerted by its addition to Portland

* Corresponding author. Tel.: +34 91 3020440; fax: +34 91 3026047.
E-mail address: nuriah@ietcc.csic.es (N.H. Rodríguez).

0008-8846/$ – see front matter © 2009 Elsevier Ltd. All rights reserved.
doi:10.1016/j.cemconres.2009.11.012

cement on the hydration, water demand, setting and mechanical strength of standardized mortars.

2. Experimental

The concentration of major elements in the sludge was determined by X-ray fluorescence using a Philips PW1404 X-ray spectrometer, with a Sc-Mo tube, and four analyzer crystals: PX-1, GE, LIF200, LIF220; the working conditions were 40 kV and 70 mA. The concentration of minority elements in the sludge was determined with a Thermo Jarrel ASH ICP-AES instrument, while the total C was found with a Leco furnace. Loss on ignition at 1000 °C was determined, using a muffle furnace.

The composition of the organic matter in the sludge was analyzed via thermochemolysis, which entails simultaneous methylation and thermal degradation. The instruments used included a Fischer 0316 Curie point pyrolyser with a Curie temperature of 590 °C attached to a Fisons GC8000 gas chromatographer, in turn coupled to a Fisons MD800 mass spectrometer. GC was conducted under the following conditions: oven temperature: 50 °C for 1 min, ramped to 280 °C at a rate of 5 °C/min., and thereafter to 320 °C at 30 °C/min; carrier gas: helium at a constant flow rate of 1 ml/min.; interface temperature: 280 °C; chromatographic column: ZB-5 ms, 30 m × 0.25 mm × 0.25 μm; injector temperature 280 °C; type of ionization: electron impact at an energy of 70 eV, source temperature: 250 °C.

Fatty acids were saponified and extracted from the sample for direct injection into the gas chromatographer. A standardized protocol (MIDI) was used to analyze the components of the bacterial cell walls. The conditions were the same as in the preceding procedure, with the following exceptions: oven temperature: 80 °C for 4 min, ramped to 120 °C at a rate of 30 °C/min., subsequently to 260 °C at 5 °C/min and finally to 310 °C at 40 °C/min.; carrier gas: helium at a constant flow rate of 1.50 ml/min.

Thermal behaviour was studied with differential thermal and thermogravimetric analysis, heating specimens at a rate of 4 °C/min. to a maximum temperature of 1050 °C in N_2 and air. A TA Instruments SATQ600 apparatus was used. In addition, the atomized sludge was heated at 500 °C for 30 min, after which XRD and FTIR techniques were used to characterize the product obtained, whose total carbon was also determined.

The atomized sludge sample was mixed with Al2O3 (approx. 30% by weight) to quantify the amorphous material content via Rietveld refinement analysis of XRD data. LXRPD data have been recorded with an X'Pert MPD PRO diffractometer (Philips) using CuKα_1 radiation ($\lambda = 1.5406$ Å), [Ge(111) primary monochromator]. The optics configuration was a fixed divergence slit (1/2°), a fixed incident anti-scatter slit (1°), a fixed diffracted anti-scatter slit (1/2°) and an X'Celerator RTMS (Real Time Multiple Strip) detector, working in scanning mode with maximum active length. The data were collected from 5° to 70° (2θ) during ~2 h. The samples were rotated during data collection at 15 rpm in order to enhance particle statistics. The X-ray tube worked at 45 kV and 35 mA.

Ten FTIR scans were performed on KBr (1 mg of sample/300 mg KBr) pellets at frequencies of from 4000 to 400 cm^{-1} and a spectral resolution of 4 cm^{-1} with a Thermo Scientific Nicolet 600 spectrometer.

The environments in which the Si and Al atoms were found in the sludge were studied with nuclear magnetic resonance of both nuclei. ^{29}Si and ^{27}Al solid state NMR spectra were obtained with a Bruker NLS-400 spectrometer operating at 79.49 and 104.26 MHz, respectively, using MAS techniques and 4-μs π/2 pulses, a 5-s pulse delay, and spinning speeds of 4 and 12 kHz. A total of 800 and 200 scans were obtained, respectively, for the ^{29}Si and ^{27}Al spectra. The standards used to adjust chemical shift in the ^{29}Si and ^{27}Al nuclei were tetramethylsilane (TMS) and a 1 M solution of $AlCl_3 \cdot 6H_2O$, respectively.

Specific surface was measured with N_2 absorption-desorption isotherms, using the BET method and a Micrometrics Asap 2000 volumetric apparatus. Particle size distribution was determined with laser ray diffraction (Helos 12LA Sypatec) using dry feed systems and a measuring range of from 0.1 to 1750 μm. Sludge morphology and structure were studied under a JEOL model JSM-5400 scanning electron microscope fitted with an OXFORD EDX apparatus and ISIS LINK software.

Sludge pozzolanicity was evaluated by conducting the pozzolanic activity test set out in Spanish and European standard UNE-EN 196-5. This involved blending I 42.5 R/SR type cement and sludge in a proportion of 75/25; 20 g of this blend were added to 100 cm^3 of water and stored in a closed flask at 40 °C for seven days. After that time the Ca^{2+} and OH^- ion concentrations in the solution were analyzed and the results plotted on the portlandite saturation curve.

Four I 42.5 N/SR cement/sludge blends were prepared, with ratios by weight of 90/10, 80/20, 75/25 and 70/30. Water demand and setting of the cement/sludge blends were determined pursuant to standard UNE-EN 196-3; the same materials were used to make prismatic standardized mortar specimens measuring 40 × 40 × 160 mm to determine 2- and 28-day compressive and bending strength. The slump was also determined (standard UNE-EN 196-1) in the fresh mortar.

The heat of hydration generated by I 42.5 N/SR cement and the blended ones 90/10 and 70/30, was monitored with a TA Instruments THAM AIR conduction calorimeter, under the following conditions: $T = 25$ °C; binder weight = 5 g; mixing water weight = 2 g. I 42.5 N/SR and the blended ones 90/10 and 70/30, hydrated pastes of various ages, were treated at different times with acetone to detain hydration and then characterized for mineralogy using X-ray diffraction (XRD) and IR spectroscopy (FTIR) techniques.

3. Results

3.1. Chemical composition

Table 1 gives the chemical composition of the atomized sludge, obtained with XRF (major elements), ICP (minor elements) and Leco (carbon).

The four major oxides identified were silicon, aluminium, calcium and iron. The sample had a very high alkali content, particularly Na_2O and the P_2O_5 concentration was around 1% by weight. The loss on ignition at 1000 °C (22.7%) included the loss of moisture and organic matter, dehydroxylation of phyllosilicates, decarbonation of carbonates and so on.

The total ion chromatogram for the sludge contained alkane and alkene peaks, but primarily composed fatty acids with chain lengths in the C_{12}–C_{22} range. The acids, which appeared in the form of their methylated derivatives, were attributed to the presence of such compounds in the sample. The presence of alkanes and alkenes may be due to the thermal degradation of the fatty acids themselves during analysis, conducted at temperatures at which fatty acids would be decarboxylated to yield the respective alkanes and alkenes with one less carbon atom. Saponification generated cleaner chromatograms with clearly separated fatty acids (Fig. 1).

Table 1
Chemical composition of atomized sludge expressed in oxides. XRF (major elements), ICP (minor elements) and Leco (carbon) elemental analysis.

Oxide (% by weight) (XRF)				Oxide (ppm) (ICP)			
SiO_2	29.63	SO_3	0.34	BaO	435.4	PbO	<10.77
Al_2O_3	17.57	K_2O	2.85	CdO	<2.28	ZnO	186.71
Fe_2O_3	5.18	TiO_2	0.56	Co_3O_4	12.25	ZrO	65.78
MnO	0.15	P_2O_5	0.94	Cr_2O_3	62.84	B_2O_3	482.99
MgO	2.15	Cl (sol)	0.16	CuO	61.33	As_2O_3	72.22
CaO	11.85	LI*	22.70	MnO	1200.85	V_2O_5	339.19
Na_2O	6.09			NiO	64.89	Sb_2O_3	1.91
C (Leco)	5.10					P_2O_5	9739.18

LI: loss on ignition at 1000 °C.

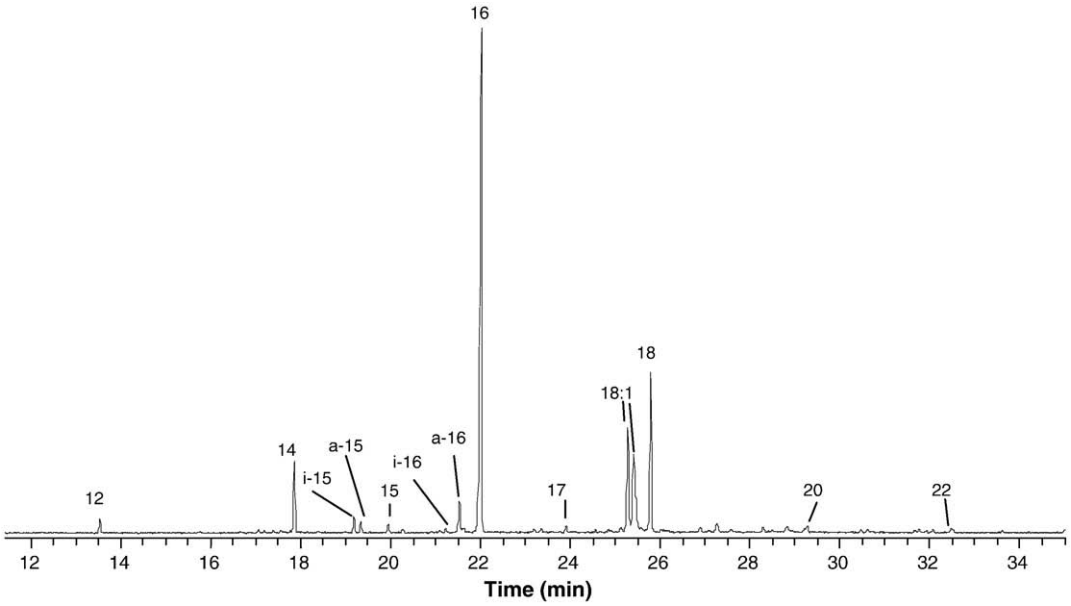

Fig. 1. Chromatogram for saponified M2 sludge. $n \rightarrow$ number of carbon atoms in the fatty acid chain; the prefixes i- and a- indicate iso-branched y anteiso-branched.

3.2. Mineralogy

Fig. 2 shows the X-ray diffractogram of the atomized sludge and Table 2 the quantitative analysis of crystalline phases and amorphous content. The main crystalline phase was muscovite, while the amorphous component accounted for 35.2% (w/w).

The medium intensity band at around 3617 cm^{-1} on the FTIR spectrum for the atomized sludge (Fig. 3) was attributed to the ν_1 vibrations generated by the hydroxyl groups in the silicates, while the wide band at 3441 cm^{-1} was assigned to the same vibrations generated by the O–H bonds in water. The bending vibrations due to the H–O–H in the water appeared at 1649 cm^{-1}. The ν_3 and ν_2 stretching bands generated by the C–O groups in the calcite appeared at around 1434 and 875 cm^{-1}. The bands at 1160, 1080, 793 and 778 cm^{-1} (double band) were attributed to the stretching vibrations from the Si–O bonds in the quartz. The intense band peaking at around 1030 cm^{-1}, the shoulder at lower wave numbers (912 cm^{-1}), along with the intense bands at 528 and 470 cm^{-1} and the above-mentioned bands at 3617 and 3441 cm^{-1}, were assigned to illite–montmorillonite [24]. No dolomite bands were clearly visible in the spectrum.

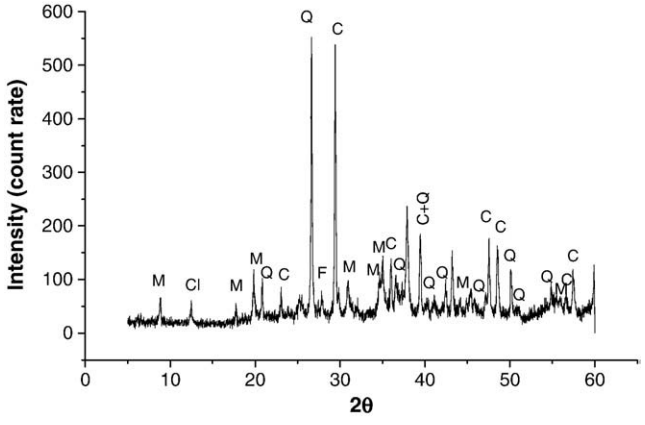

Fig. 2. Atomized sludge sample diffractogram. Q = quartz; C = calcite; M = mica; Cl = chlorite ; F = feldspar.

3.3. Thermal behaviour

Fig. 4 shows the N_2 and air DTA/TG thermograms for the atomized sludge. Sample mass declined from 80 to 900 °C regardless of the working atmosphere. Total mass loss in air was 24.3% and in N_2, 25.6%. This difference may be due to sample heterogeneity or to oxidation of the air sample.

The DTA curves for the sludge in air and N_2 (Fig. 4) had two endothermal signals with minima at 112 and 760 °C, respectively attributed to the loss of moisture and hydration water in organic matter the first and the thermal decomposition of carbonates and water loss in mica the second. According to Mackenzie's studies [28] on two natural muscovites, dehydroxylation began at 700 °C in this mineral, which lost around 4.5% of its weight between 700 and 950 °C.

The air DTA also exhibited a strong exothermal signal peaking at 305 °C that was absent in the N_2 graph and was due to the combustion of the organic matter in the material; the mass loss associated with this peak amounted to 11%.

The carbon content in the sludge determined after incineration for 30 min at 500 °C, was 2.19% (w/w). Given that organic matter combustion is produced about 300 °C that carbon is assigned to calcite and dolomite phases in the sludge.

3.4. Si and Al environments studied with ^{29}Si and ^{27}Al MAS NMR

Fig. 5 shows the ^{29}Si and ^{27}Al MAS NMR spectra for atomized sludge.

The large spinning sidebands and wide central band (width = 22 ppm) on the ^{29}Si spectra were attributed to the presence of

Table 2
Atomized sludge mineralogy (% by weight) obtained by Rietveld refinement.

Chemical formula	Name	Content
$(K,Na)(Al,Mg,Fe)_2(AlSi_3O_{10})(OH)_2$	Muscovite	25.9 (4)
$(Mg_5Al)(Si_3Al)O_{10}(OH)_8$	Chlorite	4.6 (2)
$CaMg(CO_3)_2$	Dolomite	3.1 (1)
$(Na,K)AlSi_3O_8$	Anorthoclase	2.3 (2)
SiO_2	Quartz	11.6 (1)
TiO_2	Anatase	0.5 (1)
$CaCO_3$	Calcite	16.7 (1)
Amorphous		35.2 (5)

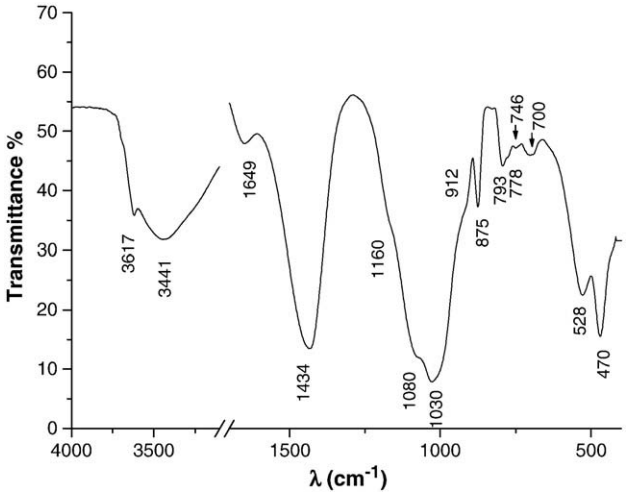

Fig. 3. Atomized sludge FTIR spectra.

paramagnetic iron. The chemical shift in the central band (−85 ppm) concurred with previous reports for muscovite [26,28]. Sanz and Serratosa [25] attributed the three bands (−81, −85 and −89 ppm) resolved in mica samples with low iron contents to Si($SiAl_2$); Si(Si_2Al) and Si(Si_3), respectively. These same authors [33] resolved up to five signals between −74.5 and −93.5 ppm in synthetic micas with different charges (Na-n micas, $n=2, 3, 4$). The band at around −106 was due to the quartz in the sample (Si(4Si)). ^{29}Si NMR bands from $NaKAlSi_3O_8$ would be in the interval between −92 and −104 ppm [29].

The ^{27}Al spectrum had two bands, the more intense at 4.63 ppm (75% of Al), characteristic of octahedrally coordinated Al and the other peaking at 69.60 ppm, with a shoulder at 57.69 ppm, both characteristic of tetrahedrally coordinated Al (25% of Al). Sanz et al. [25] place the octahedral band in muscovite at 1.5 ppm [28], Mackenzie [28] at around 0 ppm, Woessner [30] at 3.5 ppm; Welch [31], in turn, places the octahedral band in seraphinite at 8.3 ppm. The tetrahedral Al band also had two components: one at 69.6 ppm interpreted to be due to the Al that replaces the Si in the tetrahedral layer of mica [25,32,33] and in seraphinite [31] and the other at 57.69 characteristic of the Al replacing the Si in the three-dimensional structure of feldspars [27].

3.5. Mean particle size and BET specific surface

The specific weight of the atomized sludge was 2.2 g/cm^3 and its mean particle size was 23.84 μm. The diameter of 90% of the particles was under 50 μm. The BET specific surface area of the sludge was 3.29 m^2/g; the mean desorption pore diameter was 22.09 nm while microporosity was 0.0209 cm^3/g.

3.6. Morphological characterization

The existence of different particle sizes in the atomized sludge can be observed in the SEM microphotograph in Fig. 6. As the figure shows, the particles were primarily round and poorly crystalline, although many were covered with laminar or annular structures.

3.7. Study of the pozzolanic capacity of sample atomized sludge

The analysis of the pozzolanicity test solution (UNE-EN 196-5) showed it to contain [OH] = 102 mmol/l and [CaO] = 4.11 mmol/l. When we represent these values on the CaO–OH diagram, they are on the saturation curve of portlandite. Consequently, the test did not provide conclusive results on the possible suitability of atomized sludge as an active pozzolanic addition.

3.8. Hydration of cement-atomized sludge

Fig. 7 shows the variation in heat during hydration in three pastes (I 42.5 N/SR cement, 90/10 and 70/30 cement-DWTPS blended cements) and Table 3 gives data taken from the calorimetric curves.

The heat of hydration curve for the cement paste was characterized by an intensely exothermal first signal (not completely recorded) due to the initial dissolution and hydrolysis of the cement phases. This was followed by a period of scant thermal activity and subsequently by the intermediate hydration phase and a concomitant rise in the rate of heat release (acceleration period). The rate later declined during the deceleration period, which gave way to the steady state or diffusion period [34].

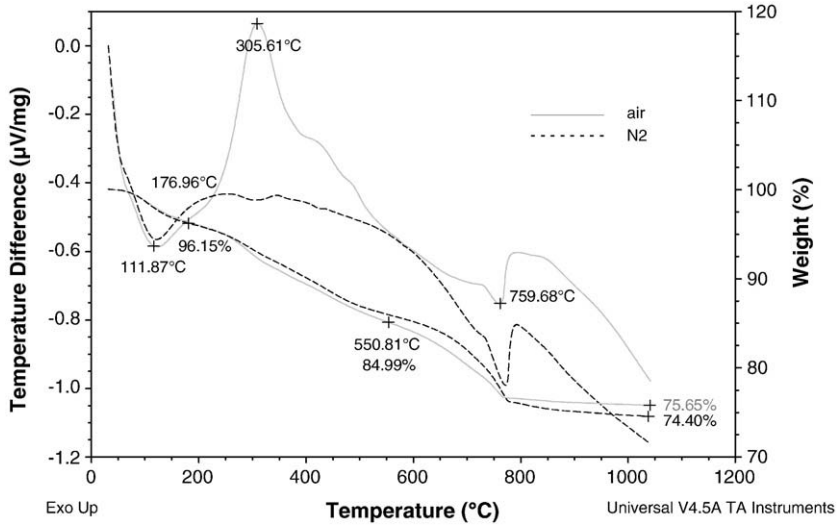

Fig. 4. DTA/TG thermograms for the atomized sludge.

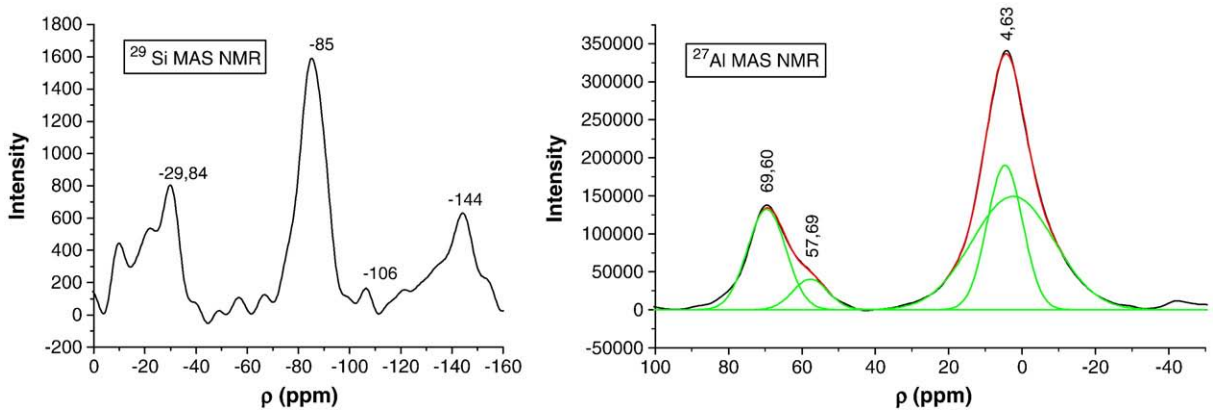

Fig. 5. ^{29}Si and ^{27}Al MAS NMR spectra for the atomized sludge.

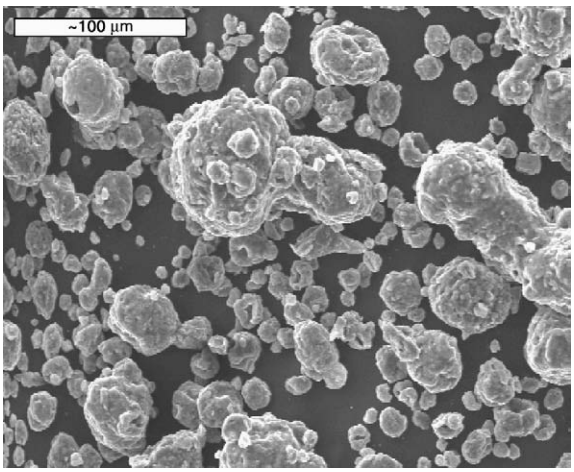

Fig. 6. SEM microphotograph showing rounded and poorly crystalline particles of different sizes in the atomized sludge.

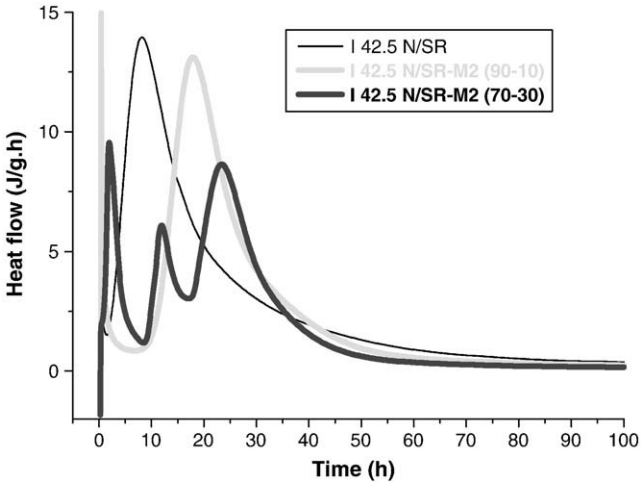

Fig. 7. Conduction calorimetry curves showing heat evolution in the three pastes.

Replacing 10% of the cement with sludge M2 lengthened both the induction period (by 6 h) and the time when maximum heat release was recorded. The total heat released after 160 h declined by 15% with respect to the unadditioned cement, but only by 6% when the value was expressed in J/g of cement.

Replacing 30% of the cement with sludge altered the heat flow curve significantly. Three exothermal signals were recorded, with values as shown in the Table 3. The third signal, which can be clearly attributed to the acceleration and deceleration periods of cement hydration, appeared at much later times than in the preceding two samples. The other two signals were more difficult to interpret. The first peaked at 2 h, by which time the induction period had ended in the cement without sludge addition. This could be an indication that the addition retarded initial cement dissolution due to the hydrophobic fatty acids [35]. Alkali ions from atomized sludge could also react with fatty acids [35] or inhibit the normal hydration of calcium silicates lengthening the induction period [36]. One of these two initial signals might also be generated by bassanite hydration, and the attendant formation of gypsum or ettringite. The total heat released by this sample after 160 h was lower than in the cement with no additions, but when dilution was taken into consideration and the value expressed in J/g of cement, the difference was only 1.5%.

In order to identify the processes giving rise to the aforementioned signals, hydration was interrupted with acetone in the 70/30 pastes at shorter times and the specimens were studied under XRD and FTIR. Fig. 8 shows the FTIR spectra for 70/30 pastes hydrated for six (after the first peak), 15 (after the second peak) and 24 (at the beginning of deceleration) hours, as well as for the 70/30 anhydrous blend.

The absence of the characteristic portlandite band in both the six and the fifteen-hour spectra indicated that the pastes were still in the induction period and portlandite nucleation had not begun. The main difference between the anhydrous spectrum sample and the sample hydrated for 6 h appeared in the sulfate area, at around 1100 and 600–700 cm^{-1}. The shape of the bands at the higher wave numbers changed and the bands at 660 and 600 cm^{-1} disappeared. Furthermore, a new band was observed at 617 cm^{-1}, which remained visible on the 15- and 24-hour spectra. The band reflecting the cement silicates (at 927 cm^{-1}) overlapped with the sludge band in the

Table 3
Induction period, maximum heat flow and heat released in 160 h in the three pastes.

	Induction per.		Max heat flow				Heat (J/g) after 160 h	
	End t (h)		t (h)		(J/g h)		J/g mix	J/g cem.
I 42.5N/SR	2		8.2		13.96		294.3	294.3
90/10 cem.-sludge	8.4		17.9		13.11		249.7	277.4
70/30 cem.-sludge	1st peak		2nd peak		3rd peak			
	t(h)	J/gh	t(h)	J/gh	t(h)	J/gh	203	289
	2	9.54	12	6.1	23	8.6		

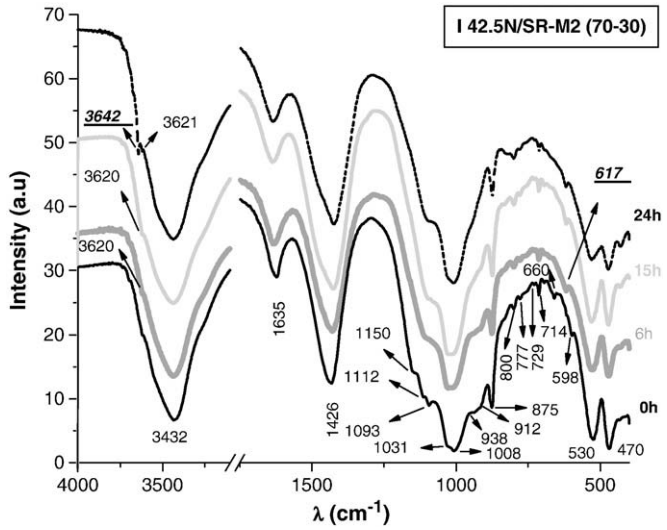

Fig. 8. I 42.5N/SR-M2 sludge blends: spectra for anhydrous material and pastes hydrated for 6, 15 and 24 h.

anhydrous cement spectrum. While it remained unchanged after 6 h, it declined after 15 and much more after 24 h.

Fig. 9 shows the XRD patterns for the 70/30 anhydrous sample and the pastes hydrated for 6, 15 and 24 h.

These patterns confirmed the FTIR findings regarding the absence of portlandite in the six and the fifteen-hour pastes, providing further evidence that the pastes were still in the induction period and no portlandite nuclei had yet formed.

The main difference between the diffractograms for the anhydrous and the 6-hour hydrated sample consisted in the slight increase in the intensity of the muscovite peaks.

No changes were observed in the silicate, aluminate, ferrite or sulfate peaks, nor were any new peaks present that would denote the presence of ettringite. The changes observed in the FTIR spectra in the sulfate area were not confirmed by the XRD findings, inferring that the sulfate phase obtained was either amorphous or below the detection threshold for this technique.

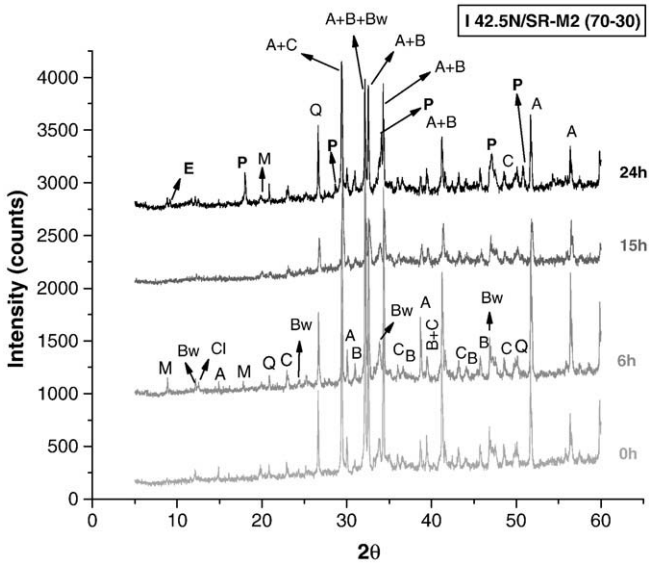

Fig. 9. I 42.5N/SR-M2 sludge blends. XRD patterns for the anhydrous material and pastes hydrated for 6, 15 and 24 h. A = alite; B = belite; Bw = brownmillerite; C = calcite; Q = quartz; P = portlandite; Cl = chlorite; M = muscovite; E = ettringite.

Table 4
Water demand for standard consistency and initial and final setting times for cement/sludge blends.

Cement	Consistency		Setting time	
	Water (g)	Consist. (mm)	Initial	Final
I 42.5 R/SR	177	33	4 h 35′	6 h 5′
90% I 42.5 R/SR + 10% F*	220	33	4 h 40′	8 h 25′
80% I 42.5 R/SR + 20% F*	208	33	13′	1 h 13′
75% I 42.5 R/SR + 25% F*	207	34	1 h 7′	6 h 30′
70% I 42.5 R/SR + 30% F*	183	36	2 h 12′	14 h 12′

F:atomized sludge.

Table 5
Mortar slump and strength activity index (SAI).

	SAI (%)	Slump (mm)
I 42.5 R/SR	100.00	52.25
90% I + 10% F*	40.79	24.5
80% I + 20% F*	52.62	2
75% I + 25% F*	35.32	21.75
70% I + 30% F*	29.31	36.5

F: atomized sludge.

The 15-h diffractogram exhibited a slight decline in the intensity of the silicate, aluminate and ferrite peaks, confirming the decline in the band at 938 cm^{-1} observed in the FTIR spectrum. While no portlandite or ettringite peaks were observed on this XRD trace, they were present in the 24-h diffractogram.

3.9. Physical and mechanical

Tables 4 and 5 together Fig. 10 show the effect of adding different proportions of atomized sludge to I 42.5 R/SR cement on the setting time, mechanical strength, slump and water needed to achieve standard consistency.

According to these results, adding up to 25% by weight of atomized sludge to cement substantially altered setting times and increased water demand, even in blends in which the addition accounted for only 10% by weight of the total. Although the increase in water demand in the blend with 30% sludge was moderate, false setting was observed in these specimens.

At the same time, both 2- and 28-day flexural strength and compressive strength declined with increasing atomized sludge content in the mortar.

4. Discussion

To manage the waste generated at drinking water treatment plants (DWTPs), it has been used a new experimental treatment process by atomization that reduces sludge volume 600-fold and converts it to a readily handled powdery material that might be reusable in the cement or concrete industry [2].

The rounded shape of the atomized sludge together with its mean particle size (smaller than the mean particle size in SSA [3], but similar to the Portland cement) would initially make the atomized sludge compatible with cement for the use described. Nonetheless, this sludge would be expected to be less reactive than many of the SSAs cited in the literature [12,37,38] in light of its lower BET specific surface value.

Further to the DTA/TG results, at up to 550 °C, the weight loss in the atomized sludge was 14% (w/w). Since at that temperature all the organic matter burns off and since moisture loss was found to be 2–4%,

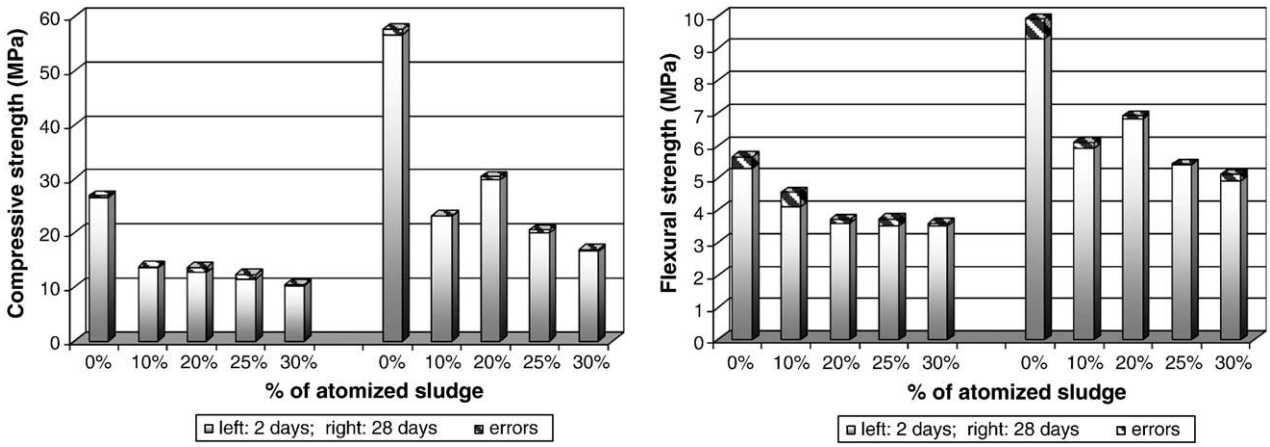

Fig. 10. Compressive and flexural strength.

the maximum amount of organic matter was 10–12%, with an organic carbon content of 2.9%. With a proportion of organic matter much lower than in other types of atomized sludge (38% of dry weight [21]) used as components in mortar and concrete, the atomized sludge studied here would be expected to have less of an impact on the physical and mechanical properties of such materials.

According to the chromatograms obtained via both thermochemolysis and saponification (Fig. 1), fatty acids where the majority components of organic fraction in the sludge. The pattern observed is compatible with the presence of a build-up of the microbial biomass that forms the sludge [39]. Indeed, analyses of the fatty acids in water containing a substantial population of microorganisms yields similar results (Lichtfouse et al. 1995), and the fatty acid profiles reported for wastewater sludge [40,41] are likewise similar. Gram-negative microorganisms are characterized mainly by a high abundance of C16:0 in their mass spectra. On the other hand, gram-positive microorganisms contained a high abundance of branched C15:0 (iso or anteiso) in their mass spectra [41,42].

The major crystaline phase in the atomized sludge was mica, followed by calcite, quartz and chlorite. Literature on the subject reports the presence of quartz in SSA, while some authors also identified phosphorus salts (hydroxylpatite and whitlockite), feldspars, mica and calcite. Cyr et al. [3] determined a vitreous content (40%) much higher than identified by XRD in this study (35%), bearing in mind that the latter figure included 10–12% of organic matter. Other authors [43,44] have reported vitreous contents of 60–70%.

A comparison of the chemical composition of the atomized sludge to the mean composition of different types of SSA [3] revealed that the proportion of $SiO_2 + Al_2O_3$, i.e., the most active components in the pozzolanic reaction, was close to the mean value. The main differences lie in loss on ignition, four times higher in this case, the P_2O_5 percentage (nine times lower) and the Na_2O content (six times higher).

With reference to the heavy metal content in this atomized sludge, the concentration of Cd, Co, Cu, Ni, Pb, Sb and Zn was much lower than the minimum values reported by Cyr for SSA [3], while As, Ba, Cr were much lower and vanadium higher.

Pozzolanic activity is related to composition (high SiO_2 and Al_2O_3 contents favour such activity) but also to the structure of a material: the more amorphous, the more active. In general, silicon is found in pozzolans as part of a vitreous or amorphous material or in crystalline zeolites. Silicon usually forms part of a three-dimensional network (Si Q4) in which SiO4 tetrahedra are often replaced by AlO4 tetrahedra.

Pursuant to the NMR results, most of the Si in the atomized sludge was found in the tetrahedral phyllosilicate layer. This layer is fairly stable and scantly reactive with portlandite. At the same time, 75% of the Al was observed to be in octahedral units, which are less favourable to pozzolanic activity than tetrahedral units.

The Frattini test was not conclusive with respect to atomized sludge pozzolanicity. The high concentration of hydroxyl ions is related to the high alkali content in sludge ($Na_2O = 6.06\%$ and $K_2O = 2.85\%$), which raises the pH of the solution, which was saturated in portlandite.

The partial replacement of cement with sludge led to substantial retardation of hydration rates, even in the 90/10 samples, which would explain their lower 24-hour strength. Replacement of larger proportions of cement (sample 70/30) significantly altered the initial hydration stages, lengthening the induction period by over 12 h and prompting the hydration of the bassanite and sulfoaluminate formation. The latter compound has some FTIR bands in a similar position to ettringite but was X-ray amorphous. In the 70/30 sample, in turn, silicate hydration was perceptibly retarded, possibly due to a reaction between the fatty acids and the Ca^{2+} and OH^- ions in the medium, which would inhibit portlandite nucleation. High alkali atomized sludge content could also contribute to delay the calcium silicate hydration process [36].

Replacing cement with atomized sludge altered setting behaviour (and in the 70/30 blend even caused a false set [46]) and occasioned a substantial decline in the slump of standardized mortars, which was not directly proportional to the replacement percentage.

The mechanical strength of the standardized mortars also declined substantially, even when only 10% of the cement was replaced with atomized sludge. The strength activity index (SAI) (Table 5), which relates the 28-day compressive strength of mortars made with cement containing different percentages of sludge additions to the strength of the control, declined with increasing proportions of sludge at all ages, in a proportion much higher than the percentage replacement of cement. These results proved that the atomized sludge failed to behave like either an active addition or an inert substance. The significant decline in mortar performance and the setting alterations may be related to the organic matter in the atomized sludge.

According to Albayrack et al. [45], the presence of fatty acids retards setting time and lowers strength by up to 50%. They attributed the steep decline observed in compressive strength to the fragility of the double bonds present in fatty acid structures, which are readily oxidized during the curing period by the oxygen dissolved in the water, causing microscopic fissures.

Other authors observed longer cement setting and lower hydration rate in the presence of fatty acids, with intense alterations in initial ettringite formation. This has been explained by the hydrophobic effect of the acids when bonding to cement particles [35].

The strength of mortars was much lower than reported by others working with SSA [3,5,8,15]. However, these experiments were conducted with dry sludge ash after incineration at temperatures of up to 1000 °C, which eliminates the organic matter and destroys crystalline structures, generating an artificial pozzolan.

Studies realized on concrete carrying non-incinerated sewage sludge report that the presence of sludge reduces substantially the mechanical strength of concrete recommending additions of 10% or less and only for certain specific uses [23].

5. Conclusions

1- The material generated by spray drying DWTP sludge is a readily handled powder which had a rounded form and a particle size similar to that observed in Portland cement, and a BET specific surface one order of magnitude higher.
2- Atomized sludge contained 12–14% organic matter, 2–4% moisture, muscovite (25.9%), quartz (11.6%), calcite (16.7%), dolomite (3.1%) and seraphinite (4.6%), anortoclase (2.3%) and 35% amorphous material. The heavy metal content (except vanadium) in this atomized sludge was much lower than in sewage sludge ash.
3- In the atomized sludge studied, the proportion of $SiO_2 + Al_2O_3$, i.e., the most active components in the pozzolanic reaction, was similar to the mean value reported in the literature for SSA, although the sludge structure was essentially crystalline and exhibited no activity in the Frattini trial or when it was tested for alkali activation.
4- The partial replacement of cement by sludge led to substantial retardation of hydration rates, even in the 90/10 samples. Replacement of larger proportions of cement significantly altered initial hydration, lengthening the induction period by over 12 h, and silicate hydration was perceptibly retarded. A reaction between the fatty acids and the Ca^{2+} and OH^- ions in the medium, would inhibit portlandite nucleation.
5- The mortars made with type I 42.5 R/SR Portland cement mixed with 10 to 30% atomized sludge exhibited a substantial decline in slump and lower mechanical strength than the control cement, with 28-day strength activity index values of 30 to 50%. Setting was also altered in the blended cements with respect to the control.
6- According FTIR results the presence of fatty acids in the mixes atomized sludge/cement can induce amorphous ettringite formation.

Acknowledgements

This study was conducted under the leadership of Aguas de Barcelona as part of a CENIT (National Strategic Consortia for Technical Research) project titled “Technological development for a self-sustainable urban water cycle” (SOSTAQUA), funded by the Spanish Centre for Technological Development in Industry (CDTI). Authors thanks to Dr. Cesáreo Sáiz Jiménez and Dr. Bernardo Hermosín for the help in the chromatographic studies.

References

[1] EUROSTAT, http://epp.eurostat.cec.eu.int.2005.
[2] Patent nº ES2157752 (A1) “Procedimiento de obtención de un producto pulverulento a partir de la fracción de rechazo de una planta potabilizadora de agua, producto obtenido con tal procedimiento y utilización de tal producto”. 2002, (http://lp.espacenet.com/publicationDetails/originalDocument?CC=ES&NR=2157752A1&KC=B1&DB=lp.espacenet.com&locale=es_LP).
[3] M. Cyr, M. Coutand, P. Clastres, Technological and environmental behavior of sewage sludge ash (ssa) in cement-based materials, Cement and Concrete Research 37 (2007) 1278–1289.
[4] J. Monzó, J. Payá, M.V. Borrachero, A. Córcoles, Use of sewage sludge ash (ssa)–cement admixtures in mortars, Cement and Concrete Research 26 (1996) 1389–1398.
[5] J. Monzó, J. Payá, M.V. Borrachero, E. Peris-Mora, Mechanical behavior of mortars containing sewage sludge ash (ssa) and portland cements with different tricalcium aluminate content, Cement and Concrete Research 29 (1999) 87–94.
[6] S.C. Pan, D.H. Tseng, C.C. Lee, C. Lee, Influence of the fineness of sewage sludge ash on the mortar properties, Cement and Concrete Research 33 (2003) 1749–1754.
[7] C.H. Chen, I.J. Chiou, K.S. Wang, Sintering effect on cement bonded sewage sludge ash, Cement and Concrete Composites 28 (2006) 26–32.
[8] E.G. Alcocel, P. Garces, J.J. Martínez, J. Payá, L.G. Andión, Effect of sewage sludge ash (ssa) on the mechanical performance and corrosion levels of reinforced portland cement mortars, Materiales de Construccion 56 (2006) 31–43.
[9] J.-H. Tay, Reclamation of wastewater and sludge for concrete making, Resources, Conservation and Recycling 2 (1989) 211–227.
[10] M.H. Al Sayed, I.M. Madany, A.R.M. Buali, Construction and Building Materials 9 (1995) 19–23.
[11] J. Monzó, J. Payá, M.V. Borrachero, I. Girbés, Reuse of sewage sludge ashes (ssa) in cement mixtures: the effect of ssa on the workability of cement mortars, Waste Management 23 (2003) 373–381.
[12] K.S. Wang, I.J. Chiou, C.H. Chen, D. Wang, Lightweight properties and pore structure of foamed material made from sewage sludge ash, Construction and Building Materials 19 (2005) 627–633.
[13] I.J. Chiou, K.S. Wang, C.H. Chen, Y.T. Lin, Lightweight aggregate made from sewage sludge and incinerated ash, Waste Management 26 (2006) 1453–1461.
[14] H.L. Luo, D.F. Lin, Study the surface color of sewage sludge mortar at high temperature, Construction and Building Materials 21 (2007) 90–97.
[15] P.A. Garcés, M.A. Pérez Carrión, E.B. García-Alcocel, J. Payá, J. Monzó, M.V. Borrachero, Mechanical and physical properties of cement blended with sewage sludge ash, Waste Management 28 (2008) 2495–2502.
[16] V. Zivica, Resistance of cement mortars containing heavy metal oxides exposed to long-term repeated action of chloride solution, Construction and Building Materials 10 (1996) 515–519.
[17] X.D. Li, C.S. Poon, H. Sun, I.M.C. Lo, D.W. Kirk, Heavy metal speciation and leaching behaviors in cement based solidified/stabilized waste materials, Journal of Hazardous Materials 82 (2001) 215–230.
[18] R. Cenni, B. Janisch, H. Spliethoff, K.R.G. Hein, Legislative and environmental issues on the use of ash from coal and municipal sewage sludge co-firing as construction material, Waste Management 21 (2001) 17–31.
[19] I. Fernández Olmo, E. Chacon, A. Irabien, Influence of lead, zinc, iron (III) and chromium (III) oxides on the setting time and strength development of Portland Cement, Cement and Concrete Research 31 (2001) 1213–1219.
[20] P.H. Shih, J.E. Chang, H.C. Lu, L.-C. Chiang, Reuse of heavy metal-containing sludges in cement production, Cement and Concrete Research 35 (2005) 2110–2115.
[21] S. Valls, E. Vàzquez, Stabilization and solidification of sewage sludges with portland cement, Cement and Concrete Research 30 (2000) 1671–1678.
[22] S. Valls, E. Vàzquez, Accelerated carbonation of sewage sludge-cement-sand mortars and its environmental Impact, Cement and Concrete Research 31 (2001) 1271–1276.
[23] S. Valls, A. Yagüe, E. Vázquez, C. Mariscal, Physical and mechanical properties of concrete with added dry sludge from a sewage treatment plant, Cement and Concrete Research 34 (2004) 2203–2208.
[24] K. Oinuma, H. Hayashi, Infrared study of mixed- layer clay minerals, The American Mineralogist 50 (1965).
[25] J. Sanz, J.M. Serratosa, ^{29}Si and ^{27}Al High-Resolution MAS NMR Spectra of phyllosilicates, Journal of the American Chemical Society 106 (1984) 4790–4793.
[26] R.A. Kinsey, R.J. Kirkpatrick, J. Hower, K.A. Smith, E. Oldfield, High-Resolution ^{27}Al and ^{29}Si Nuclear Magnetic-Resonance Spectroscopic study of layer silicates, including clay-minerals, American Mineralogist 70 (1985) 537–548.
[27] R.J. Kirkpatrick, R.A. Kinsey, K.A. Smith, et al., High resolution solid-state ^{23}Na, ^{27}Al, and ^{29}Si nuclear magnetic resonance spectroscopic reconnaissance of alkali and plagioclase feldspars, American Mineralogist 70 (1985) 106–123.
[28] K.J.D. Mackenzie, I.W.M. Brown, C.M. Cardile, et al., The thermal reactions of muscovite studied by high-resolution solid-state ^{29}Si and ^{27}Al NMR, Journal of Materials Science 22 (1987) 2645–2654.
[29] K.L. Geisinger, R. Oestrike, A. Navrotsky, et al., Thermochemistry and structure of glasses along the join $NaAlSi_3O_8$–$NaBSi_3O_8$, Geochimica et Cosmochimica Acta 52 (1988) 2405–2414.
[30] D.E. Woessner, Characterization of clay minerals by ^{27}Al nuclear magnetic-resonance spectroscopy, American Mineralogist 74 (1989) 203–215.
[31] M.D. Welch, J. Barras, J. Klinowski, A multinuclear NMR-study of clinochlore, American Mineralogist 80 (1995) 441–447.
[32] S. Komarneni, R. Pidugu, J.E. Amonette, Synthesis of Na-4-mica from metakaolinite and MgO: characterization and Sr^{2+} uptake kinetics, Journal of Materials Chemistry 8 (1998) 205–208.
[33] M.D. Alba, M.A. Castro, M. Naranjo, et al., Hydrothermal reactivity of Na-n-micas ($n = 2, 3, 4$), Chemistry of Materials 18 (2006) 2867–2872.
[34] I. Jawed, J. Skalny, J.F. Young, Hydration of portland cement, in: P. Barnes (Ed.), Structure and performance of cements, Applied science publishers, London, 1983.
[35] E.E. Hekal, M. Abd-El-Khalek, G.M. El-Shafey, F.S. Hashem, Mechanical and physicochemical properties of hardened portland cement pastes containing hydrophobic admixtures: Part 1. Compressive strength and hydration kinetics, ZKG International 52 (12) (1999) 697–700.
[36] A. Palomo, A. Fernández-Jiménez, G. Kovalulchuck, L.M Ordoñez, M.C Naranjo, OPC-Fly ash cementititious systems: study of gel binders produced during alkaline hydration, Journal of Materials Science 42 (2007) 2958–2966.
[37] S.C. Pan, D.H. Tseng, Sewage sludge ash characteristics and its potential applications, Water Science and Technology 44 (2001) 261–267.
[38] C.M.A. Fontes, M.C. Barbosa, R.D. Toledo Filho, J.P. Goncalves, Potentiality of sewage sludge ash as mineral additive in cement mortar and high performance concrete, International Rilem Conference on the use of Recycled Materials in Buildings and Structures, vol. 8–11, 2004, pp. 797–806.

[39] E. Lichtfouse, G. Berthier, S. Houot, E. Barriuso, V. Bergheaud, T. Vallaeys, Stable carbon isotope evidence for the microbial origin of C_{14}–C_{18} *n*-alkanoic acids in soils, Organic Geochemistry 23 (1995) 849–852.

[40] E. Ibañez, S. Borros, L. Comellas, M. Gassiot, Determination of B-hydroxy fatty acids in sewage sludge by using selected ion monitoring, Journal of Chromatography A 775 (1997) 287–293.

[41] F. Basile, K.J. Voorhees, T.L. Hadfield, Microorganism gram-type differentiation based on pyrolysis-mass spectrometry of bacterial fatty acid methyl ester extracts, Applied and Environmental Microbiology 61 (1995) 1534–1539.

[42] A. Conrad, M. Kontro, M.M. Keinänen, A. Cadoret, P. Faure, L. Mansuy-Huault, J.C. Block, Fatty acids of lipid fractions in extracellular polymeric substances of activated sludge flocs, Lipids 38 (2003) 1093–1105.

[43] T.D. Dyer, J.E. Halliday, R.K. Dhir, Hydration reaction of sewage sludge ash for use as a cement component in concrete production, recycling and reuse of sewage sludge, Proceeding of the International Symposium, vol. 19–20, 2001, pp. 227–238.

[44] M.A. Anderson, M.B. Elliott, C.C. Hickson, Factory-scale proving trials using combined mixtures of three by product wastes (including incinerated sewage sludge ash) in clay building bricks, Journal of Chemical Technology and Biotechnology 77 (2002) 345–351.

[45] A.T. Albayrak, M. Yasar, M.A. Gurkaynak, I. Gurgey, Investigation of the effects of fatty acids on the compressive strength of the concrete and the grindability of the cement, Cement and Concrete Research 35 (2005) 400–404.

[46] I. de la Cruz, T. Vázquez, O. Fernández-Peña, Sulfatos en el cemento portland y su incidencia en el falso fraguado: estado actual del conocimiento, Materiales de Construcción 192 (1983) 43–55.